Observation of antiferromagnetic interlayer exchange coupling in a $Ga_{1-x}Mn_xAs/GaAs:Be/Ga_{1-x}Mn_xAs$ trilayer structure

J. Leiner,[1,*] H. Lee,[2] T. Yoo,[2] Sanghoon Lee,[2,†] B. J. Kirby,[3] K. Tivakornsasithorn,[1] X. Liu,[1,‡] J. K. Furdyna,[1] and M. Dobrowolska[1]

[1]*Department of Physics, University of Notre Dame, Notre Dame, Indiana 46556, USA*

[2]*Department of Physics, Korea University, Seoul 136-713, Korea*

[3]*Center for Neutron Research, NIST, Gaithersburg, Maryland 20899, USA*

(Received 6 September 2010; published 16 November 2010)

Interlayer exchange coupling (IEC) between two $Ga_{0.95}Mn_{0.05}As$ layers separated by Be-doped GaAs spacers was investigated experimentally using magnetization, magnetotransport and neutron-scattering measurements, which all indicated the presence of robust antiferromagnetic IEC when the GaAs spacer is sufficiently thin. We argue that the observed behavior arises from a competition between the interlayer exchange field and magnetocrystalline anisotropy fields intrinsic to GaMnAs layers.

DOI: 10.1103/PhysRevB.82.195205 PACS number(s): 75.50.Pp, 61.05.fj, 61.72.uj, 75.70.Cn

I. INTRODUCTION

The study of ferromagnetic (FM) dilute magnetic semiconductors (DMSs) continues to be of great interest because of their potential for spin-electronic device applications.[1] While there has been much progress in our understanding of DMS materials—particularly of the canonical III-V system $Ga_{1-x}Mn_xAs$ (Ref. 2)—many issues still remain unresolved. One of these issues is the nature of interlayer exchange coupling (IEC) in GaMnAs-based multilayers. Here it is particularly important to establish whether the IEC between adjacent GaMnAs layers is antiferromagnetic (AF) or FM since manipulation of such IEC can serve as the basis for a wide range of devices.

Theoretical models predict that both FM and AF IEC can occur in GaMnAs multilayers, the type of coupling depending on the thickness and doping of the spacers between the FM layers.[3–6] So far, however, experimental studies have shown predominantly FM IEC,[7–9] while AF IEC has only recently been observed in superlattices comprised of GaMnAs layers and GaAs:Be spacers.[10] To address this issue, a study of two GaMnAs layers separated by a nonmagnetic GaAs spacer is particularly useful since such a trilayer enables one to "zoom in" on the specific properties of GaMnAs that determine the IEC. It is especially important to explore the coupling between GaMnAs layers with different spacer properties.[11] We have therefore investigated a series of GaMnAs-based trilayer samples using magnetotransport measurements, superconducting quantum interference device (SQUID) magnetometry, and neutron scattering. In all these independent studies we have observed clear evidence of AF IEC between the two GaMnAs layers in the case when the spacer between the layers is sufficiently thin and when it is doped by Be to a sufficiently high level.

II. SAMPLE PREPARATION

The GaMnAs/GaAs:Be/GaMnAs trilayers used in this study were grown by molecular-beam epitaxy (MBE) on (100) GaAs substrates at 250 °C, by first growing a $Ga_{0.95}Mn_{0.05}As$ layer to a thickness of 17.2 nm (bottom layer), then a GaAs spacer doped by Be (doping level estimated as $10^{20}-10^{21}$ cm^{-3}, based on the temperature of the Be cell), and finally a $Ga_{0.95}Mn_{0.05}As$ layer 8.6 nm thick (top layer). The series consisted of trilayers with different spacer thicknesses ranging from 4.3 to 17.2 nm and different spacer dopings. A diagram of the sample structures is shown in Fig. 1(a).

III. EXPERIMENTAL RESULTS AND DISCUSSION

SQUID measurements were used to measure the temperature dependence of the trilayer magnetization $M(T)$. Magnetization data for the trilayer with a 4.3 nm spacer and an

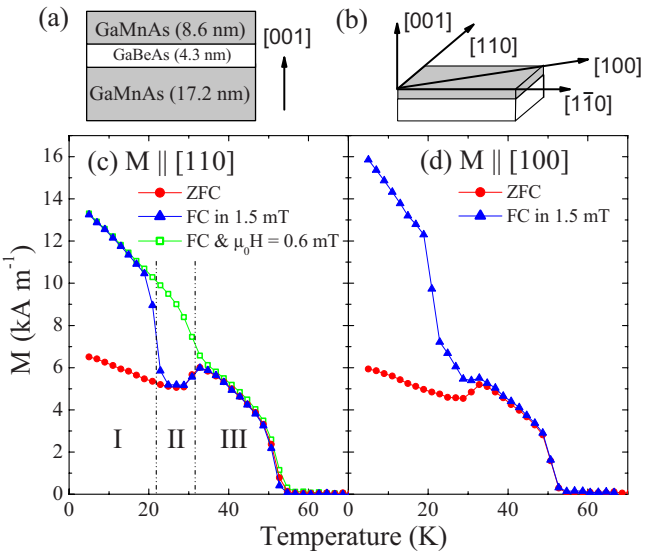

FIG. 1. (Color online) (a) The structure of the trilayer samples grown by MBE. (b) The coordinate system used in this work. [(c) and (d)]: temperature dependence of remnant magnetization in a trilayer sample with respect to [110] and [100] crystallographic directions. The data were collected while warming with no applied field, after cooling from 200 to 5 K in either zero field or 1.5 mT. Also shown in (c) is FC data measured in an applied field of 0.6 mT.

average hole concentration over the entire trilayer of 2×10^{20} cm^{-3} are shown in Figs. 1(c) and 1(d). The sample was oriented so that the measured magnetization and the applied field **H** were parallel to either the uniaxial easy axis [110] or to the cubic easy axis [100] [see Fig. 1(b)] of the GaMnAs layers.[12] The sample was either field cooled (FC) in a field of 1.5 mT, or zero field cooled (ZFC), and the magnetization was then measured as the temperature was increased in zero field. As shown in Figs. 1(c) and 1(d), three distinct behaviors are observed in three different temperature regimes. Below 20 K the FC and ZFC data differ dramatically, where FC leads to a conspicuous enhancement of the magnetization for both field directions, and a suppression of magnetization is observed in ZFC data. We attribute these characteristics to a parallel alignment (addition) or an antiparallel alignment (subtraction) of **M** of the two GaMnAs layers. Moreover, a clear dip in $M(T)$ is observed for the FC data around 30 K, with a minimum in Fig. 1(c) corresponding exactly to the ZFC value of M at the same temperature, suggesting that the parallel alignment of **M** of the GaMnAs layers at low temperature in the FC case switches to antiparallel alignment as T exceeds ~20 K. Note, however, that when the temperature dependence of **M** is measured in a finite field [0.6 mT in Fig. 1(c)], the FC data do not show this dramatic dip, indicating that the presence of a small applied field prevents the AF reorientation from occurring. Finally, above 30 K the $M(T)$ curves for FC and ZFC are seen to merge both for measurements along the [110] and the [100] directions, first increasing, and then decreasing as T increases. In this temperature region the value of M suggests that only one GaMnAs layer (bottom) contributes to $M(T)$, as discussed later in the paper. Thus the magnetization data in Fig. 1 show clear signs of AF IEC.

Polarized neutron reflectometry (PNR) provides further evidence for AF IEC. An incident neutron beam was polarized alternately parallel (spin-up) or antiparallel (spin-down) to a magnetic field **H** applied along the [110] GaMnAs direction, and the nonspin-flip specular reflectivity was measured as a function of scattering vector Q_z along the sample normal. The neutron beam was monochromatic (0.475 nm wavelength, less than 1% spread), and polarized with greater than 91% efficiency. Corrections were applied to the data to account for the beam footprint and background. No significant off-specular or spin-flip scattering from the sample was detected. The lack of spin-flip scattering (which arises from the in-plane magnetization component perpendicular to **H**) is not surprising, as model calculations demonstrate[13,14] that the weak GaMnAs magnetization is insufficient to produce any easily detectable spin-flip scattering, regardless of orientation. The spin-up and spin-down nonspin-flip specular reflectivities are sensitive to the depth profiles of the nuclear composition and the in-plane magnetization parallel to **H**.[13,14] Thus, we were able to use model fitting of the nonspin-flip data with exact dynamical calculations[14] to confirm the AF IEC and determine the actual magnetizations of the individual GaMnAs layers within the trilayer structure.

After cooling to 5 K in zero field, a small field (<1 mT) was applied to ensure polarization of the neutron beam, and PNR spectra were measured to determine the spontaneous (i.e., ZFC) magnetization state of the trilayer. To probe the field-dependent evolution of the magnetic profile, PNR measurements were then taken at 20 mT, and then taken below 1 mT after cycling the field between +800 and −800 mT. An additional PNR measurement was taken at 800 mT to establish the saturation profile. The fitted PNR data corresponding to the spontaneous and saturation magnetic states are compared in Fig. 2. In panels (a) and (b), the fitted data are shown multiplied by Q_z^4 (the intensity falloff for a smooth interface). For both field conditions, the reflection critical edge is evident as a peak in both spin states near 0.115 nm^{-1}. The sample magnetization causes the critical edge to be in slightly different positions for the two neutron polarization states. For clarity of presentation, we choose to define "spin up" as the neutron polarization state that gives the larger critical Q_z, and "spin down" as the neutron polarization state that gives the smaller critical Q_z. There are clear spin-dependent oscillations in the scattering that are significantly different for the spontaneous and saturation states. For the spontaneous state, the spin splitting is more pronounced at higher Q_z than near the critical edge while this trend is reversed for the saturation state.

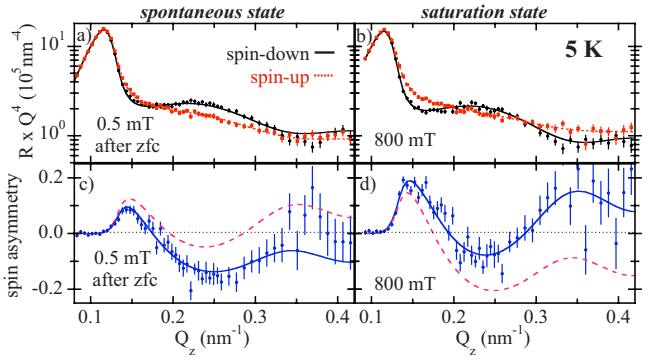

FIG. 2. (Color online) Fitted polarized neutron reflectometry data plotted as [(a) and (b)] $R \times Q_z^4$ and [(c) and (d)] as spin asymmetry. [(a) and (c)] Data corresponding to the "spontaneous" magnetic state are shown on the left and [(b) and (d)] that corresponding to the "saturation" state are shown on the right. In low field after ZFC, the spin splitting is more pronounced at higher Q_z than it is near the critical edge, indicating antiparallel alignment of the top and bottom GaMnAs layers. Error bars correspond to $\pm 1\sigma$.

These spin dependencies are highlighted by recasting the fitted data as spin asymmetry[15,16] (the difference in spin-up and spin-down reflectivities divided by their sum), as shown in Figs. 2(c) and 2(d). The best fits to the data [solid lines in Figs. 2(c) and 2(d)] reveal that the spontaneous state corresponds to antiparallel alignment of the top and bottom GaMnAs layer magnetizations while the saturation state corresponds to parallel alignment. The dashed lines in Figs. 2(c) and 2(d) are fits corresponding to the best-fit models with the top layer magnetizations reversed (i.e., spontaneous parallel alignment and antiparallel alignment at saturation). The alternate profiles clearly result in a significantly worse fit to the data than do the best-fit models, indicating our sensitivity to the orientations of the individual GaMnAs layers.

The depth profiles corresponding to the best fit to the data are shown in Fig. 3. Panel (a) shows the nuclear composition profile used to fit all of the data in terms of the nuclear

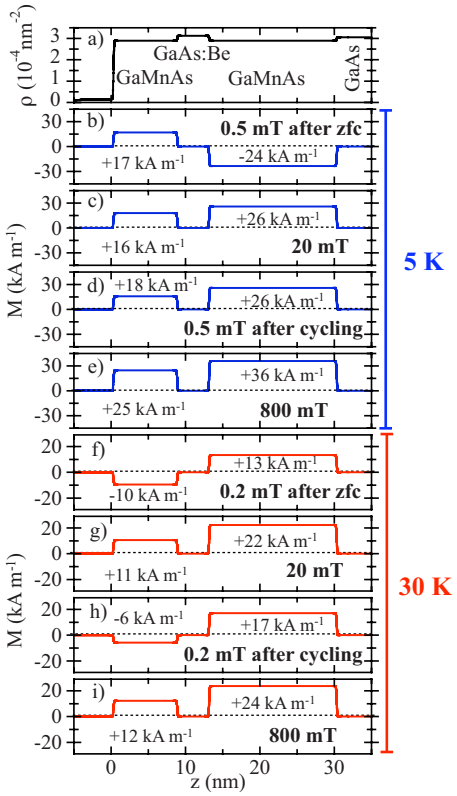

FIG. 3. (Color online) Depth profiles used to fit the PNR data: (a) nuclear profile, [(b)–(e)] 5 K magnetic profiles, and [(f)–(i)] 30 K magnetic profiles. The length z in the horizontal axis is measured from the top of the sample.

scattering length density ρ. (Note that for the 5 K data, a low ρ surface layer was allowed to vary in composition and thickness from field to field, in order to account for a small amount of time-dependent gas condensation on the sample surface.) There is little nuclear contrast among the layers but the GaMnAs is distinguishable from the GaAs:Be spacer and GaAs substrate by a reduced ρ. The 5 K magnetization depth profiles are shown in panels (b)–(e). (b) The top and bottom GaMnAs layers spontaneously align antiparallel, (c) align parallel upon application of 20 mT, and (d) remain in the parallel configuration in 0.5 mT after cycling. The above procedure was repeated for PNR measurements at 30 K, and the resulting magnetic profiles are shown in Figs. 3(f)–3(i). Spontaneous antiparallel alignment is again observed [Fig. 3(f)] but in this case the antiparallel alignment is recovered after field cycling, attesting to a more robust AF IEC at this temperature. These results are similar to what has previously been observed for a GaMnAs/GaAs:Be superlattice.[10] Thus, despite the difference in the respective boundary conditions characteristic of the trilayer and the superlattice geometrics,[6] both systems behave in a qualitatively similar fashion, i.e., both exhibit competing effects of AF IEC and magnetocrystalline anisotropy. For completeness we also used PNR to measure the saturation magnetization of the layers at 800 mT at 30 K and 40 K, where the results were M_{top}= +12 kA m^{-1}, M_{bot}=+24 kA m^{-1} and M_{top}=+11 kA m^{-1}, M_{bot}=+20 kA m^{-1}, respectively, indicating that the Curie temperatures of both bottom and top layers are above 40 K.

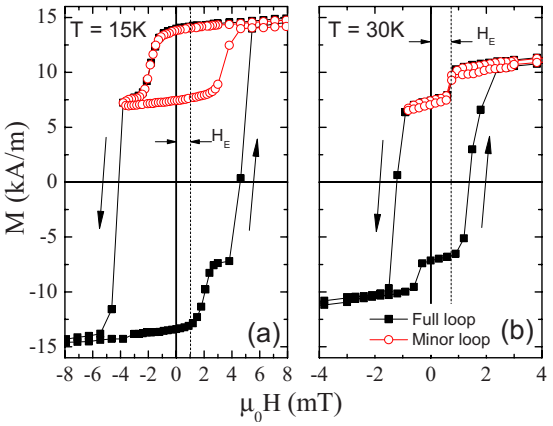

FIG. 4. (Color online) Magnetization curves for field along the [110] direction taken at different temperatures. (a) T=15 K and (b) T=30 K. Filled and empty symbols show the full and minor loops, respectively.

Further insight into IEC can be gained by examining the hysteresis loops of the trilayer at different temperatures (Fig. 4). The hysteresis curves show a two-step magnetization reversal both at 15 and 30 K. The fact that the top GaMnAs layer is half as thick as the bottom layer allows us to attribute the smaller loop to the top layer. The 15 K loop shows a decreasing magnetization step only after the field has been swept past zero to −2 mT. In contrast, the magnetization curve at 30 K clearly shows the reversal of magnetization of the top GaMnAs layer occurring *before* the field reaches zero, indicating robust AF alignment that returns after cycling to saturation, very similar to what was seen in the PNR data. Qualitatively we can picture this as the top layer "feeling" an exchange bias field H_E from the bottom layer that acts to accelerate the reversal of magnetization *even before* reaching zero field. Moreover, note that the minor hysteresis loop in Fig. 4(b) is centered to the right of H=0, from which we can infer that at 30 K the value of H_E is ~0.73 mT. A closer inspection of Fig. 4(a) shows that the minor hysteresis loop for 15 K is also centered to the right of H=0, shifted by ~0.85 mT. This indicates that H_E is also present at that temperature—in fact it is stronger than at 30 K—but is overshadowed by the much larger coercive field at the lower temperature.

The PNR and $M(H)$ data which confirm the presence of AF IEC also enable us to better interpret the behavior of $M(T)$ in Fig. 1. This can be understood by considering the relative strengths of the coercive field associated with magnetocrystalline anisotropy and the interlayer exchange field H_E at different temperatures. It is well known that the cubic anisotropy field H_C decreases very rapidly with increasing temperature while the uniaxial anisotropy field H_U decreases much more slowly. The temperature dependence of H_E is unknown but based on our results we will argue that H_E falls off faster with increasing temperature than H_U, and more slowly than H_C. Thus, based on our results we suggest that, as the temperature increases, the mechanism dominating the hysteresis loop changes from the cubic anisotropy field H_C to interlayer exchange H_E, and finally to the uniaxial anisotropy field H_U. As seen in Fig. 1(c), at ~22 K the magnetization

of FC data undergoes a precipitous drop, consistent with a transition between dominance by H_C (where the coercive field is larger than H_E) and IEC dominance (where the coercive field is smaller than H_E). In our trilayer this dominance of H_E prevails in only a short temperature range since by the time the sample reaches 30 K, the effect of uniaxial anisotropy H_U appears to overcome the contributions of both H_E and H_C, as discussed below.

We now comment on our inability to observe IEC at higher temperatures (>33 K). It has been shown previously that the magnetic properties of GaMnAs depend on the electronic properties (e.g., on doping) of the layer on which it is grown,[17,18] and that the resulting increased hole concentration in GaMnAs can result in switching of the uniaxial easy axis by 90°, from [110] to $[1\bar{1}0]$.[19,20] Since in the present case the top layer of the sample was grown on a heavily Be-doped spacer, it is possible that above a certain temperature the top GaMnAs layer experiences a reorientation of magnetization *perpendicular* to that of the bottom layer. In this situation the magnetizations of the two GaMnAs layers are orthogonal, and the contribution of the top layer to the magnetization (which was seen to reduce the total ZFC magnetization in Fig. 1 at low temperatures due to AF coupling) now disappears. This would explain the increase in $M(T)$ just above 30 K of both FC and ZFC data in Fig. 1. One should note here that the differences between the low-temperature FC and ZFC SQUID magnetizations as well as their increase (of 15–20 %) just above 30 K are very close to the respective values of M obtained by PNR (see Fig. 3), thus corroborating the model used in fitting the PNR results.

For magnetotransport measurements the trilayer was patterned into a Hall bar in the form of a rectangular strip 200 μm long and 10 μm wide, as shown in the inset in Fig. 5(a), with gold wires attached to each terminal by indium contacts. The current through the Hall bar was along the [110] direction. The sample was mounted in a 4 K cryostat such that a magnetic field **H** could be applied in the plane of the sample. Magnetoresistance (MR) was measured at various azimuthal angles ϕ_H of the applied field [see inset in Fig. 5(a)]. The characteristics of MR as a function of applied field **H** in thin GaMnAs films are well known.[7,21,22] In particular, the in-plane MR data typically shows a two-horn pattern, where the two kinks result from the switching of the direction of magnetization at the coercive field. This feature is observed in our trilayer at 4 K, where the magnetization switching in both layers occurs simultaneously [see Fig. 5(a)]. Note, however, that at the beginning of the measurement (immediately following ZFC), the resistance is higher than at any later time. The high resistance seen in this first sweep is the result of the antiparallel alignment of magnetizations of the two GaMnAs layers after ZFC, i.e., before cycling,[7,23] consistent with the 5 K ZFC SQUID and with the neutron data obtained at 5 K (already shown). At 30 K the robust AF IEC which occurs at this temperature is manifested as a distinct upward jump in MR appearing before the applied field returns to zero after cycling, as seen in Fig. 5(b). This increase in resistance due to a spontaneous reorientation of M to antiparallel alignment suggests the potential for device applications of such magnetic semiconductor structures.

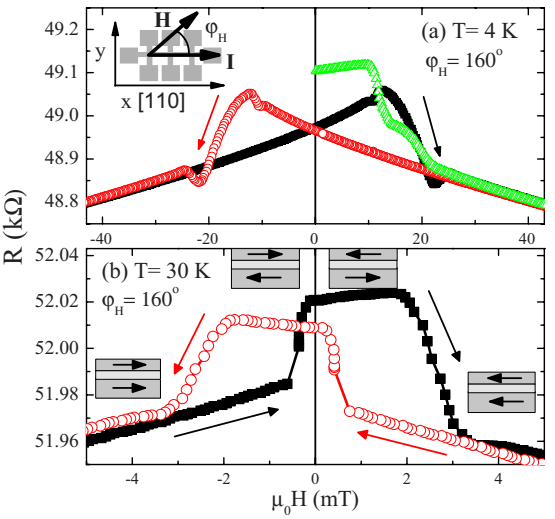

FIG. 5. (Color online) (a) Field-dependent sheet resistance in a trilayer sample at 4 K after zero field cooling. (b) Field-dependent sheet resistance at 30 K, after zero field cooling. Sketches show the configuration of the magnetizations at the indicated points on the resistance plot. The directions of the arrows are along the uniaxial easy axis [110] of GaMnAs. Inset of (a): Hall bar pattern. H is the applied magnetic field and I is the applied current.

IV. CONCLUSION

In summary, our experiments conclusively show the existence of AF IEC in a GaMnAs/GaBeAs/GaMnAs trilayer. We have observed that the relative orientation of **M** in the two layers is determined by the competition between an interlayer exchange coupling and magnetic anisotropy intrinsic to GaMnAs. We have observed AF IEC in a sample with layer thicknesses of 8.6/4.3/17.2 nm (30/15/60 monolayers). This is somewhat surprising since recent theoretical studies[6] predict that—while AF coupling is possible for trilayer samples with spacers comparable to ours—the magnetic layers should not be thicker than a few monolayers for the effect to occur. Trilayers containing spacers with greater thicknesses and lower Be doping in our sample series showed no sign of AF IEC. These results provide insights for further experiments aimed at understanding the exchange interaction in between GaMnAs layers.

ACKNOWLEDGMENTS

This work was supported by the NSF under Grants No. DMR06-03762 and No. DMR10-0581; by a NSF EAPSI under Grant No. OISE-0914013; and by Mid-career Researcher Program through NRF grant funded by the MEST under Grants No. 2010-0025880 and No. 2009-0085028.

*jleiner@nd.edu
†slee3@korea.ac.kr
‡xliu2@nd.edu

[1] H. Ohno, Science **281**, 951 (1998).
[2] T. Jungwirth, J. Sinova, J. Masek, J. Kucera, and A. H. MacDonald, Rev. Mod. Phys. **78**, 809 (2006).
[3] T. Jungwirth, W. A. Atkinson, B. H. Lee, and A. H. MacDonald, Phys. Rev. B **59**, 9818 (1999).
[4] P. Sankowski and P. Kacman, Phys. Rev. B **71**, 201303(R) (2005).
[5] A. D. Giddings, T. Jungwirth, and B. L. Gallagher, Phys. Status Solidi C **3**, 4070 (2006).
[6] K. Szalowski and T. Balcerzak, Phys. Rev. B **79**, 214430 (2009).
[7] D. Chiba, N. Akiba, F. Matsukura, Y. Ohno, and H. Ohno, Appl. Phys. Lett. **77**, 1873 (2000).
[8] H. Kepa, G. Springholz, T. M. Giebultowicz, K. I. Goldman, C. F. Majkrzak, P. Kacman, J. Blinowski, S. Holl, H. Krenn, and G. Bauer, Phys. Rev. B **68**, 024419 (2003).
[9] B. J. Kirby, J. A. Borchers, X. Liu, Z. Ge, Y. J. Cho, M. Dobrowolska, and J. K. Furdyna, Phys. Rev. B **76**, 205316 (2007).
[10] J. H. Chung, S. J. Chung, S. Lee, B. J. Kirby, J. A. Borchers, Y. J. Cho, X. Liu, and J. K. Furdyna, Phys. Rev. Lett. **101**, 237202 (2008).
[11] S. Lee, J. H. Chung, X. Y. Liu, J. K. Furdyna, and B. J. Kirby, Mater. Today **12**, 14 (2009).
[12] U. Welp, V. K. Vlasko-Vlasov, X. Liu, J. K. Furdyna, and T. Wojtowicz, Phys. Rev. Lett. **90**, 167206 (2003).
[13] C. F. Majkrzak, Physica B **221**, 342 (1996).
[14] C. F. Majkrzak, in *Neutron Scattering from Magnetic Materials*, edited by T. Chatterji (Elsevier Science, New York, 2005).
[15] B. J. Kirby, J. A. Borchers, J. J. Rhyne, S. G. E. te Velthuis, A. Hoffmann, K. V. ODonovan, T. Wojtowicz, X. Liu, W. L. Lim, and J. K. Furdyna, Phys. Rev. B **69**, 081307(R) (2004).
[16] B. J. Kirby, J. A. Borchers, J. J. Rhyne, K. V. ODonovan, S. G. E. te Velthuis, S. Roy, C. Sanchez-Hanke, T. Wojtowicz, X. Liu, W. L. Lim, M. Dobrowolska, and J. K. Furdyna, Phys. Rev. B **74**, 245304 (2006).
[17] T. Wojtowicz, W. L. Lim, X. Liu, M. Dobrowolska, J. K. Furdyna, K. M. Yu, and W. Walukiewicz, Appl. Phys. Lett. **83**, 4220 (2003).
[18] J. K. Furdyna, T. Wojtowicz, X. Liu, K. M. Yu, W. Walukiewicz, I. Vurgaftman, and J. R. Meyer, J. Phys.: Condens. Matter **16**, S5499 (2004).
[19] M. Sawicki, K. Y. Wang, K. W. Edmonds, R. P. Campion, C. R. Staddon, N. R. S. Farley, C. T. Foxon, E. Papis, E. Kaminska, A. Piotrowska, T. Dietl, and B. L. Gallagher, Phys. Rev. B **71**, 121302(R) (2005).
[20] S. Chung, H. C. Kim, S. Lee, X. Liu, and J. K. Furdyna, Solid State Commun. **149**, 1739 (2009).
[21] H. X. Tang, R. K. Kawakami, D. D. Awschalom, and M. L. Roukes, Phys. Rev. Lett. **90**, 107201 (2003).
[22] M. H. Jung, S. Park, J. Eom, S. H. Chun, and K. Shin, J. Appl. Phys. **104**, 083908 (2008).
[23] M. Tanaka and Y. Higo, Phys. Rev. Lett. **87**, 026602 (2001).